

Optical Characterization of Broadband Asymmetrical Quantum Well for Laser Array Application

Wei-Li Chen

National Changhua University of Education, Department of Electronic Engineering
No.1, Jin-De Road, Changhua City, Taiwan, R.O.C.
Phone: +886-4-7232105#7136 E-mail: weili@cc.ncue.edu.tw

1. Introduction

Wavelength-division multiplexing (WDM) requires multiple wavelength light sources. It is attractive to achieve multiple wavelength operation using a single substrate in wavelength-division multiplexing (WDM). Broadband characteristic is desired for components such as laser array and semiconductor optical amplifiers (SOA) used in WDM. Quantum well intermixing (QWI) [1], microarray selective epitaxy [2], and asymmetrical quantum well (AQW) design [3] have been successfully utilized to provide broaden gain spectrum. AQW design has the advantages of high reliability, simplicity in epitaxy process, and the flexibility in manipulating gain profile by arranging the number and arrangement of various wells.

2. Design and Experiment

Numerical simulation programs issued by Crosslight Software Inc. (LASTIP, PICS3D, and APSYS), were used to simulate laser characteristics. The AQWs consisted of three 6.4nm thick and five 5nm-thick compressively strained $\text{Al}_{0.065}\text{Ga}_{0.215}\text{In}_{0.72}\text{As}$ quantum wells and 9nm-thick $\text{Al}_{0.126}\text{Ga}_{0.456}\text{In}_{0.418}\text{As}$ barriers with tensile strain. There was only one quantized energy level in each well. To facilitate uniform carrier injection, the confinement energies of wide and thin quantum wells were set as 110meV and 125meV respectively. Doped 50nm thick $\text{Al}_{0.48}\text{In}_{0.52}\text{As}$ carrier blocking layers were employed outside SCH layers to reduce vertical carrier leak and enhance injection efficiency [4]. The narrow quantum wells were placed near the p-side to ease the transportation of holes in the valence band [5]. The number of wide and narrow well was determined by LASTIP simulation results in order to achieve a broad gain profile between 1.51 μm and 1.57 μm . The active region was sandwiched between parabolic 50nm-thick separate confinement heterostructure (SCH) layers. Fig.1 illustrates the band diagram of the laser structure under bias condition. The epitaxial structure was grown on n-InP substrate by Metalorganic chemical vapor deposition (MOCVD).

3. Results and Discussion

The photoluminescence (PL) spectra were measured by using a 12mW 532nm exciting laser. At 300K, as shown in Fig.2, two distinct peaks at 0.8018eV(1542nm) and 0.8297eV(1494nm) are identified and the full width at half maximum (FWHM) is 98nm. The longer tail on the higher energy side is partly contributed by 11Ln transition and other higher energy states. The dash line in Fig.2 is the spontaneous emission spectrum simulated by LASTIP. The simulated curve is normalized with respect to the higher energy peak. The result of photoreflectance (PR) performed

at 300K is shown in Fig.3. The PR transition features are compared with those of PL and simulation results. The lowest energy peak at 0.8025eV agrees with the PL low energy peak and is denoted as 11Hw. The transition feature at 0.827eV matches with high energy peak in PL spectrum and is attributed to be the ground state transition in the narrow wells, 11Hn. The third transition feature at 0.8341eV that can not be clearly resolved in PL is attributed to be the transition from the ground state in the conduction to the second level of the heavy-hole valence band in the wide wells, 12Hw. Fig. 4 illustrates that all the transition features in PL and PR shifted when the temperature is lowered from 300K to 90K. The temperature shift coefficient is 0.54nm/K. The quantitative study of the PL spectra indicated that at low temperatures, the emission was dominated by wide wells and the emission from narrow wells gradually increased when the temperature was increased.

The LIV of the Fabry-Perot (FP) laser with 250 μm cavity is shown in Fig.5. The threshold current is 24mA and the slope efficiency is 0.147W/A. The lasing gain is dominated by the narrow wells due to larger optical confinement factor, higher density of states in narrow wells, and lower mirror reflectance ($R=0.32$). The threshold current is large compared with an identical quantum well design. DFB lasers with various grating pitches (1.5~1.58 μm) are fabricated using the same substrate to verify the broadband characteristic. The distributed feedback (DFB) laser with lasing wavelength at 1518.1nm shows lower threshold current, 18mA (Fig. 6). The side mode suppression ratio (SMSR) is 26.4dB. Scanning Electron Microscopy inspection indicates that imperfect grating patterns due to process problem results in low SMSR and caused DFB lasers with lasing wavelength larger than 1540nm fail to lase. Lasing wavelength ranged from 1503nm to 1535.2nm. Fig.7 illustrates the gain profile provided by the 5nm QW only calculated by PICS3D. Given the FP lasing peak at 1515.9nm, at 1535.2nm, the gain has dropped below zero. Therefore we concluded that the gain of this channel was supported by the wide wells.

4. Conclusions

Asymmetrical MQW has been utilized for the design of DFB lasers structure to achieve the broadband characteristic. The room temperature photoluminescence spectrum width was 98nm. The details of transitions and their associated energy levels in each well were investigated by photoreflectance measurement and the results well agree with the simulation results. Although DFB lasers with wavelength larger than 1540nm failed, simulation analysis indicated that the lasing channel at 1535.2nm was supported by both narrow and wide quantum wells.

Acknowledgements

Author would like to express sincere thanks to C. C. Lee, Dr. D. Y. Lin, C. Y. Ni, and R. Xuan for their help in the lab. This research is financially supported by the National Science Council of the ROC under grant number NSC98-2221-E018-001.

References

- [1] R. Iga, T. Yamada, and H. Sugiura, *Appl. Phys. Lett.* **64** (1994) 983.
- [2] K. Kudo, Y. Furushima, T. Nakazaki, and M. Yamaguchi, *IEEE J. of Selected Topics in Quantum Electron.* **5** (1999) 428.
- [3] S. D. McDougall, O. P. Kowalski, C.J. Hamilton, F. Camacho, B. Qiu, M. Ke, R. M. De La Rue, A. C. Bryce, and J. H. Marsh, *IEEE J. of Selected Topics in Quantum Electron.* **4** (1998) 636.
- [4] J. Piprek, J. K. White, and A. J. Spring-Thorpe, *IEEE J. of Quantum Electron.* **38** (2002) 1253.
- [5] C. F. Lin, B. R. Wu, L. W. Lai, and T. T. Shih, *Optics Letters* (2001) 1099.

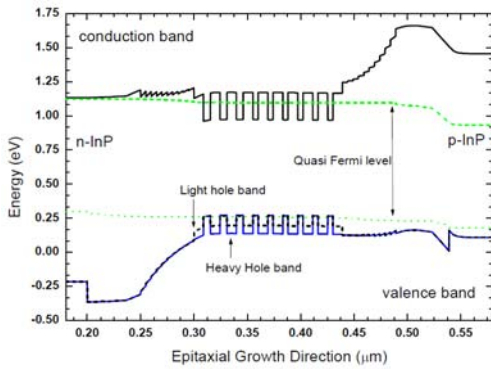


Fig.1 Band diagram of the AQW design under bias

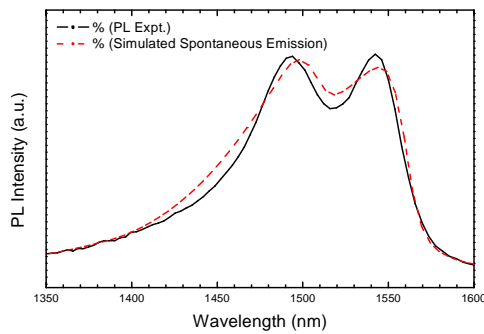


Fig.2 300K photoluminescence spectrum.

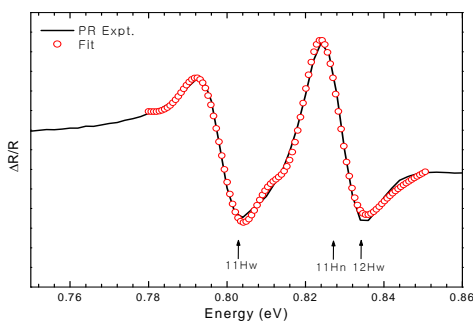


Fig.3 Photoreflectance spectrum at 300K

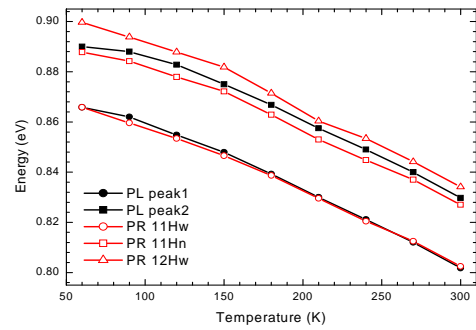


Fig.4 PL and PR peak position vs. temperature.

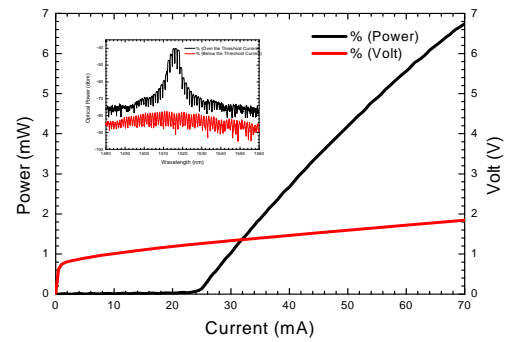


Fig.5 FP laser LIV characteristic. The optical output spectra below and above threshold are shown in the inset.

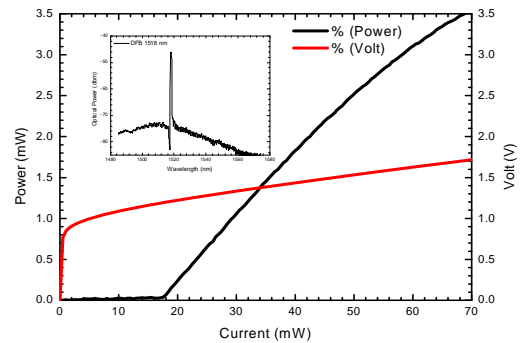


Fig.6 DFB laser LIV characteristic. The optical output spectra below and above threshold are shown in the inset.

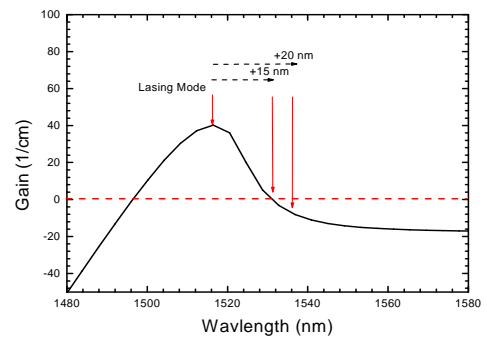


Fig.7 Gain profile of the 5nm narrow quantum well When FP lasing wavelength is 1516nm, the gain at 1535nm is negative, which indicated that DFB laser lasing at 1535nm was supported by the wide wells.